Theoretical and computational investigation of meta-phenylene as ferromagnetic coupler in nitronyl nitroxide diradicals

ARTICLE *in* THEORETICAL CHEMISTRY ACCOUNTS · FEBRUARY 2014

Impact Factor: 2.23 · DOI: 10.1007/s00214-014-1472-y

6 AUTHORS, INCLUDING:

Arun Pal
IIT Kharagpur
9 PUBLICATIONS **45** CITATIONS
SEE PROFILE

Iqbal Latif
Indian Institute of Technology Bombay
12 PUBLICATIONS **83** CITATIONS
SEE PROFILE

Sambhu N Datta
Indian Institute of Technology Bombay
128 PUBLICATIONS **941** CITATIONS
SEE PROFILE

Theor Chem Acc (2014) 133:1472
DOI 10.1007/s00214-014-1472-y

REGULAR ARTICLE

Theoretical and computational investigation of *meta*-phenylene as ferromagnetic coupler in nitronyl nitroxide diradicals

Arun K. Pal · Daniel Reta Mañeru · Iqbal A. Latif · Ibério de P. R. Moreira · Francesc Illas · Sambhu N. Datta

Received: 4 December 2013 / Accepted: 19 February 2014

Abstract We predict the magnetic exchange coupling constant (J) for 27 *m*-phenylene-based nitronyl nitroxide (NN) diradicals with nine different substituents in three unique (common *ortho*, *ortho–meta* and common *meta*) positions on the coupler unit by using the broken-symmetry density functional methodology. For all investigated diradicals, J values are computed using B3LYP, B3LYP-D3 and M06-2X functionals with 6–311+G(d,p) basis set. The $J_{\text{M06-2X}}$ value is larger than J_{B3LYP} and closer to the observed value for the unsubstituted species. Substitutions at common *ortho* position always produce a greater angle of twist between the spin source and the coupler units. When the twist angle is very large, the nature of intramolecular magnetic interaction changes from ferromagnetic to antiferromagnetic. In these cases, the coupler–NN bond order becomes small. Substitution at the common *meta* position of *m*-phenylene in the diradical has little steric and hydrogen-bonding effects. Electron-withdrawing groups reveal a specific trend for single-atom substitution. An *ortho* substitution generally decreases J and a *meta* substitution always increases J with a decreasing −I effect. Variation of J with planarity as well as Hammett constant is investigated. The nucleus-independent chemical shift value is found to decrease from the corresponding monosubstituted phenyl derivatives. The dependence of J on these factors is explored.

Keywords Diradical · Magnetic coupling constant · DFT · Dihedral angle · Inductive effect · NICS(1)

1 Introduction

Stable diradicals play an important role in research on magnetic materials of organic origin [1–3]. The intramolecular as well as the intermolecular magnetic interactions control the magnetic properties of materials [4]. The intramolecular magnetic interaction depends on the nature of the radical centers and the coupler [5–7], whereas the intermolecular interaction depends on the ground-state spin of individual molecules and the crystal structure of molecular solids [8].

In an oversimplified model, the intramolecular magnetic property of a diradical arises from the spin–spin interaction of the two unpaired electrons in two different orbitals through a (π-conjugated) spacer [6]. In case the two orbitals are near degenerate, the initial zeroth-order degeneracy of singlet–triplet total energy is lifted by electron–electron repulsion, and in case of a significant overlap between the singly occupied orbitals, the singlet lies below the triplet. This is known as the Heitler–London spin exchange between the spins of opposite sign [9]. Contrary to this, interaction between electrons in orthogonal nonbonding orbitals results in a triplet ground state. The nature of the magnetic exchange interaction, antiferromagnetic and ferromagnetic, can be predicted from the symmetry of the π-electron topology [10], starred/and non-starred rule [11], spin polarization scheme [12] and, more specifically, from

Electronic supplementary material The online version of this article (doi:10.1007/s00214-014-1472-y) contains supplementary material, which is available to authorized users.

A. K. Pal · I. A. Latif · S. N. Datta (✉)
Department of Chemistry, Indian Institute of Technology Bombay, Powai, Mumbai 400076, India
e-mail: sndatta@chem.iitb.ac.in

D. R. Mañeru · I. P. R. Moreira · F. Illas
Department de Química Física and Institut de Química Teòrica I Computacional (IQTCUB), Universitat de Barcelona, C/Martí i Franqués 1, 08028 Barcelona, Spain

Published online: 07 March 2014

spin alternation rule in the unrestricted SCF treatment [13, 14].

Thiele and Schlenk diradicals provide the classical examples of antiferromagnetic and ferromagnetic spacers, respectively [6, 15–17]. In the latter case, *m*-phenylene is the coupler unit. In fact, *m*-phenylene as a general ferromagnetic coupler is observed not only for carbon radical centers or carbenes but also for nitrogen-centered radicals such as nitroxyl and nitronyl nitroxide (NN) radicals. The aza analog of *m*-phenylene ferromagnetically couples spin sources even like transition metal ions such as Cu(II) and V(IV) [18–20].

Sometimes *meta*-phenylene acts as an antiferromagnetic coupler. The conformation of the spin source and the delocalization of spin in the substituents become responsible for this transformation. For example, Rassat et al. [21] and Iwamura et al. [22] found that the unpaired electrons of *m*-phenylene bis-(*tert*-butyl nitroxide) on hetero atoms are antiferromagnetically coupled. These authors considered that *tert*-butyl nitroxide group is twisted out of the conjugation with the *m*-phenylene linker. Iwamura et al. [22] confirmed by X-ray crystallography that the angle of twist of phenylene ring to the plane of *tert*-butyl group is 65° for syn and 75° for anti-conformations. Figure 1 shows a schematic representation of a bis-NN diradical coupled through *m*-phenylene. Borden et al. [23] have theoretically investigated the change of *m*-phenylene from a ferromagnetic coupler at a twist angle of about 0° to an antiferromagnetic one at around 90°. The change occurs due to a selective destabilization of the antisymmetric combination of singly occupied orbitals on each of the radical centers by a σ-orbital of the *m*-phenylene moiety. Mitani et al. [24, 25] have theoretically investigated polyradical systems with *m*-phenylene bridge and found high-spin ground state. Zhang et al. [26] have theoretically investigated the effect of substitution on *m*-phenylene-bridged *m*-xylene diradicals. They found that a simultaneous substitution of electron-donating and electron-withdrawing groups at *m*-phenylene and radical centers and vice versa gives rise to a singlet state or a very small S-T gap. In a recent work on *meta*-xylylene [27], we found that the hybrid B3LYP and

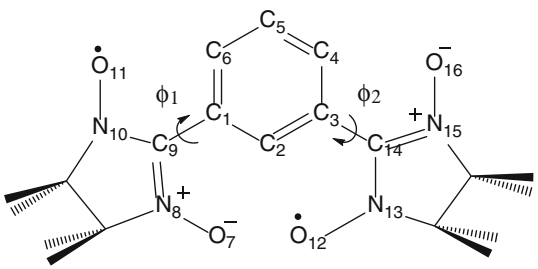

Fig. 1 Schematic representation of *meta*-phenylene bis(α-nitronyl nitroxide) or *m*-BNN

M06-2X functionals provide singlet–triplet gaps comparable to experiment. In the present work too, we will come across a few cases where the *meta*-phenylene coupler produces singlet diradicals.

The main objective of the present work is to investigate the magnetic properties of 27 substituted *m*-phenylene-based bis-NN diradicals using unrestricted density functional theory (UDFT) and the same functionals. We consider nine different substituents on the *m*-phenylene ring, namely –COOH (**1**), –F (**2**), –Cl (**3**), $-NO_2$ (**4**), –Br (**5**), –OH (**6**), $-NH_2$ (**7**), –Ph (**8**) and $-CH_3$ (**9**), in order of decreasing inductive (−I) effect (electron-withdrawing power). Each substituent occupies three unique positions, namely (**a**) common *ortho*, (**b**) *ortho–para* and (**c**) common *meta* sites on the ring (see Fig. 2). We aim to study the effect of electron attracting power of the substituents as well as the effect of the location of substituents. The role of the aromaticity of the coupler unit is also investigated. Kamiyama et al. [28] have examined the singlet–triplet energy gap of the carboxyl derivative **1c** and phenol derivative **6c** (both *common meta* variety) by continuous wave electron spin resonance (ESR) spectroscopy and static paramagnetic susceptibility measurements in the solid state. The experimental *J* values of **1c** and **6c** are $\geq -1.7\ \mathrm{cm}^{-1}$ and $\approx 8.7\ \mathrm{cm}^{-1}$, respectively, in glassy solutions of methanol. Hase et al. [29] identified the triplet ground state of **6b** (*ortho–para* variety) from the EPR measurements on the isolated molecules in diluted glassy solutions and found the *J* value of $9.0\ \mathrm{cm}^{-1}$ from magnetic susceptibility measurements in the solid state. A problem arises in these cases, as there would be extensive hydrogen bonding of the solvent hydroxyl groups not only with the substituent (COOH and OH groups) but also with the NN moieties. In solid, there would be extensive intermolecular hydrogen-bonding interactions. This is likely to have a differential effect on the relative stability of the singlet and triplet states, thereby influencing in the observed coupling constant. The experimental coupling constants would not correctly represent the coupling constants for the isolated species. The synthesis of **5c** has been accomplished by Catala et al. [7]. The unsubstituted diradical, *meta*-phenylene bis(α-nitronyl nitroxide) or *m*-BNN, has a coupling constant of $34.8\ \mathrm{cm}^{-1}$ in MeTHF [30]. To our knowledge, the other molecules have not been synthesized so far.

2 Methodology

We adopt the broken-symmetry density functional (BS-DFT) approach proposed by Noodleman et al. [31–33]. The exchange interaction between the two magnetic centers is expressed by Heisenberg spin Hamiltonian

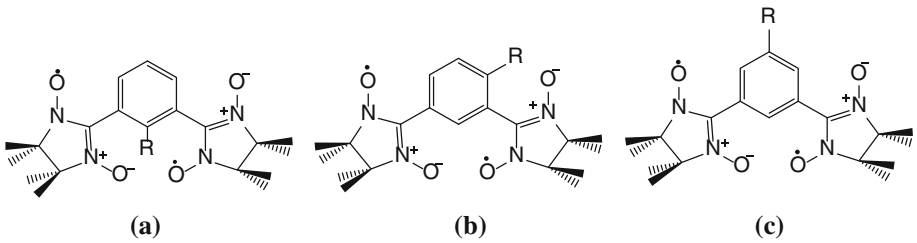

Fig. 2 The series of diradicals under investigation: R is (1) –COOH, (2) –F, (3) –Cl, (4) $-NO_2^-$, (5) –Br, (6) –OH, (7) $-NH_2$, (8) –Ph, (9) $-CH_3$

$$\hat{H} = -2J\hat{S}_1 \cdot \hat{S}_2 \tag{1}$$

where J is the magnetic exchange coupling constant. A negative value of J indicates antiferromagnetic interaction, whereas a positive value indicates the intramolecular interaction to be ferromagnetic. In the spin-projected BS approach due to Ginsberg, Noodleman and Davidson (GND), [34, 35] J can be written as

$$J^{\mathrm{GND}} = \frac{E_{\mathrm{BS}} - E_{\mathrm{T}}}{S^2_{\mathrm{max}}} \tag{2}$$

where E_{BS} is the energy of the broken-symmetry state. For a diradical, $S_{\mathrm{max}} = 1$. The spin projection technique is necessary to eliminate the spin contamination in the BS representation of the open-shell singlet. This issue has been discussed elsewhere in detail [36, 37]. In the weak overlap limit, the GND equation produces results that are comparable to the Yamaguchi equation [38, 39]:

$$J^{Y} = \frac{E_{\mathrm{BS}} - E_{\mathrm{T}}}{\langle S^2_{\mathrm{HS}} \rangle - \langle S^2_{\mathrm{LS}} \rangle}. \tag{3}$$

Here, we calculate the magnetic exchange constant using Eq. (3). Since the expectation values of the square spin operator for the high spin and broken symmetry are usually close to 2 and 1, respectively [40], this approach is almost equivalent to that obtained from the general mapping procedure allowing one to deal either with molecular or periodic systems [41].

The molecular geometries of all the 27 species in triplet state are fully optimized at ROHF/6–311G(d,p) level. In general, the ROHF/6–311G(d,p)-optimized geometries turn out to be in good agreement with the crystallographic structures [42]. ROHF with a sufficiently large basis set produces good molecular orbitals, which can be taken as initial guesses for the calculations of BS solutions at the UB3LYP, UB3LYP-D3 and UM06-2X levels using the 6–311+G(d,p) basis set. Also, a large basis set leads to a good triplet geometry. Alternatively, triplet geometry optimization can be done by UDFT methods, though we preferred ROHF for a standard and common starting point for DFT using each functional. For **5** where R = Br, the cc-PVTZ basis set is also used. The Gaussian 03 and Gaussian 09 suites of programs [43, 44] are used in the quantum chemical calculations.

To study the effect of aromaticity of the coupler on the magnetic exchange interaction, the nucleus-independent chemical shift (NICS) is calculated at the B3LYP/6–311+G(d,p) level using the GIAO methodology for all the aromatic rings in each diradical. The NICS values can be calculated at the center of the rings [NICS(0)], but since the σ framework of C–C and C–H affects the π electrons, NICS values are calculated at 1 Å above the ring [NICS(1)] where the π-electron density is generally known to be maximum [45].

Wiberg [46] bond index (order) are calculated by natural bond orbital (NBO) analysis [47, 48] at UB3LYP/6–311+G(d,p) level as implemented in Gaussian 09 [44].

3 Results and discussions

3.1 Coupling constant (J) and $\langle S^2 \rangle$ values

Computed total energy and $\langle S^2 \rangle$ values are given in Tables S1–S3 in the Supporting Information file (page 33–36). The J values calculated with B3LYP, B3LYP-D3 and M06-2X functional for all the species are given in Table 1. The coupling constant is found to follow the order **a** (common *ortho*) < **b** (*ortho–para*) < **c** (common *para*) in every case. An interesting variation of J is found for the species with substitution at the common *ortho* position for both NN fragments (**a** isomers). The calculated J varies from −2.44 to 9.3 cm^{-1}. Negative values are obtained only for **3a** and **8a**. In these cases, the ground state is an open-shell singlet, and the magnetic interaction is antiferromagnetic in nature. The maximum variation of J is found for the *ortho–para* (**b**) species. The calculated J varies from 1.9 to 18.3 cm^{-1}. The *meta* substitution (**c**) always yields a J value in the range of 18.4–24.9 cm^{-1}.

In case of the unsubstituted species, the experimental coupling constant from temperature dependence of EPR signal intensity in MeTHF is ≥34.8 cm^{-1} [30]. Our calculated J with B3LYP and B3LYP-D3 functionals are smaller, about 24 cm^{-1}, whereas M06-2X functional gives a larger value of 32.7 cm^{-1} that is in better agreement with the observed coupling constant. This trend of M06-2X giving a larger coupling constant persists for all substituted diradicals. For any functional, however, the calculated J for

Table 1 Quantum chemically calculated exchange coupling constant (J) in cm^{-1} with B3LYP B3LYP-D3 and M06-2X functionals using ROHF/6–311G(d,p)-level triplet-optimized geometry

Diradicals	6–311+G(d,p) basis set								
	J_{B3LYP}			$J_{B3LYP-D3}$			J_{M062X}		
Unsubstituted[a]	24.1			24.2			32.7		
Substituted	**a**	**b**	**c**	**a**	**b**	**c**	**a**	**b**	**c**
1	6.90	15.3	23.3[b]	6.71	15.3	23.3[b]	8.37	20.6	32.0[b]
2	9.31	12.9	21.9	9.32	13.0	23.1	12.4	17.8	31.0
3	−2.44	9.33	24.9	−2.44	9.36	25.0	−3.87	12.0	33.3
4	6.13	12.0	22.7	6.14	12.0	22.8	7.59	16.3	31.5
5	2.02	8.34	23.0	2.02	8.37	23.1	2.26	10.6	31.1
6	3.75	18.3[c]	19.9[d]	3.71	18.3[c]	19.9[d]	4.50	27.1[c]	26.3[d]
7	3.92	15.5	19.4	3.95	15.5	19.4	5.35	22.9	25.5
8	−2.74	1.89	18.4	−1.52	1.91	19.6	−2.40	2.04	26.1
9	4.89	11.0	23.6	4.91	11.0	23.6	6.12	14.6	31.7
Using cc-PVTZ									
5	2.19	8.63	23.1	2.24	8.64	23.1	2.52	11.0	31.2

[a] For the unsubstituted *m*-BNN, $J_{obs} \geq 34.8\ cm^{-1}$ in MeTHF [30]

[b] For **1c** in glassy solution of methanol, $J_{obs} \geq -1.7\ cm^{-1}$ [28]

[c] For **6b** in the solid state, $J_{obs} = 9.0\ cm^{-1}$ [29]

[d] For **6c** in glassy solution of methanol, $J_{obs} \approx 8.7\ cm^{-1}$ [28]

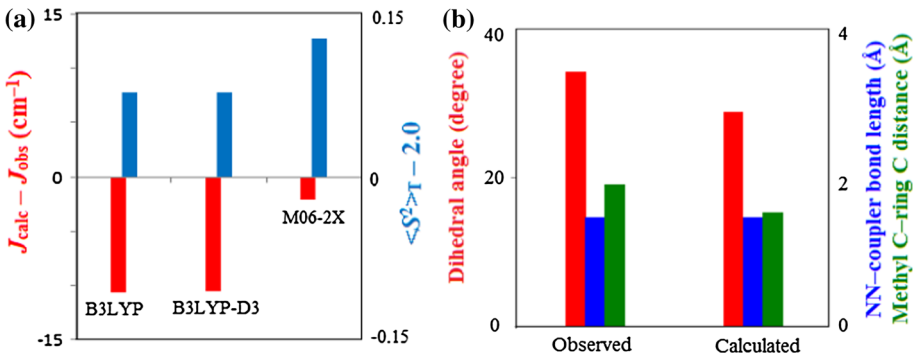

Fig. 3 **a** *Error bars* for the calculated coupling constant and the extent of spin contamination for the unsubstituted *m*-BNN. **b** Comparison of average dihedral angles, NN–coupler bond length and methyl carbon–nearest ring–carbon distance from X-ray data and ROHF optimization

the common *meta* species **c** is comparable to the calculated J for the unsubstituted *m*-BNN. As the M06-2X coupling constants for the **c** series are close to the experimental coupling constant of *m*-BNN, we use the M06-2X results for illustration except in common cases.

Figure 3a shows the error bars for the calculated J and $<S^2>_T$ of the unsubstituted *m*-BNN compared to the observed values 34.8 cm^{-1} and 2.0 a.u., respectively. Though the spin contamination in triplet is largest for M06-2X, the $\Delta<S^2>$ is approximately equal to 1 and the estimated coupling constant turns out to be nearly correct, in comparison with experiment. In Fig. 3b, we compare the critical features of the observed X-ray crystallographic geometry from Ref. [30] and the ROHF-optimized geometry used here for all functionals. The calculated average dihedral angle is 28.7° compared to the crystallographic 34.1°. The average NN–coupler bond length is 1.470(8) Å (calculated) as against 1.462(4) Å (experimental). In each NN unit, the average methyl carbon–nearest ring–carbon distance is 1.530(4) Å [ROHF/6–311G(d,p)], characteristic of a C–C single bond, whereas the crystallographic distance is 1.905 Å. The reason for the extended bond length in crystal is that the amplitude of motion of each methyl group is really large, as discussed by Shiomi et al. [30]. The error bars for all other geometrical parameters are quite small.

Unfortunately, the coupling constant for **1c** [28], **6b** [29] and **6c** [28] has been determined in glassy solution of methanol and in the solid state. These are found to be quite small, −1.7, 9.0 and 8.7 in cm^{-1}, respectively. The medium provides the scope for extensive hydrogen bonding not only with the NN radical centers but also with the substituents COOH and OH groups in the coupler, and as discussed in Introduction, cannot truly represent the coupling constants for the isolated species. The magnetic measurement on **6b** [29] in the solid state yielded the adiabatic coupling constant that has to be considerably smaller than the vertical one. The estimated M06-2X values for the isolated diradicals are 32.0, 27.1 and 26.3 cm^{-1}, respectively (Table 1).

Kitagawa et al. [49] pointed out that the spin contamination of broken-symmetry solution introduces errors in the optimized geometry and suggested the use of numerical

gradients to correct for the geometry. This aspect has been reinvestigated by Malrieu and Trinquier [50] as well as by Saito and Thiel [51]. Malrieu and Trinquier have suggested an estimation of singlet energy at each configuration and extrapolation of the geometry to obtain the minimum energy of the singlet. Saito and Thiel have derived and implemented analytical gradients for broken-symmetry unrestricted density functional calculations (BS-UDFT) with the removal of spin contamination by Yamaguchi's spin projection method. Geometry optimizations with these analytical gradients (AGAP-opt) yield results consistent with those obtained by Kitagawa et al. These techniques can be adopted to estimate the adiabatic singlet–triplet energy gap, though in this work we calculate only the vertical energy differences.

In all our calculations, the spin contamination in the triplet state is small with $<S^2>_T \sim 2.07$. For the ideal BS state, $<S^2> = 1$, and compared to this value, the spin contamination of the calculated BS states with $<S^2> \sim 1.07$ is also small ($\sim$0.07). Thus, we retrieve $\Delta<S^2> \approx 1$ that yields, in combination with good relative M06-2X energies, good estimates for the vertical coupling constant (and singlet–triplet energy gap for vertical transition) in **c** species and *m*-BNN.

3.2 Inductive effect

The decreasing trend of −I effect reveals no clear-cut systematic trend for any substituent position. Thus, electron delocalization appears to be the major factor for determining the coupling constant. For the single-atom substituents F, Cl and Br (species **2**, **3** and **5**), however, an approximate pattern emerges for the influence of inductive effect. For the common *ortho* position (**a**), the coupling constant decreases from F to Cl and Br. It becomes very small in the last two cases. However, for Cl, *J* becomes negative. For the *ortho–para* positions (**b**), the coupling constant decreases from F to Cl and from Cl to Br. For *meta* position (**c**), *J* increases from F to Cl but decreases from Cl to Br. The trends (**b**) and (**c**) can be understood from spin alternation. Any increase in electron density at the common *meta* position, as a result of substitution at *ortho–para* position, reinforces the ferromagnetic coupling due to a constructive interference of the spin wave in the coupler with the additional spin that arises from the increase in electron density by +R effect. This effect increases *J*. An increase in electron density at the *ortho* positions due to a substituent at common *meta* position leads to a destructive interference, and a smaller *J* value. The trend for (**a**) is similar to that for (**b**), but the excessively small *J* value can be attributed to the steric effect as discussed in the following. This explanation can fail in the case of a substituent with more than one atom, as the bond(s) of the substituent might be involved in delocalization, hydrogen bonding, stereo-electronic effect, etc.

3.3 Influence of planarity

The angles of rotation (ϕ_1 and ϕ_2 as in Fig. 1) of NN from the plane of the *m*-phenylene coupler are given in Table 2, which indicates that in general *J* decreases as ϕ increases. This is because the conjugation between the NN and coupler fragment decreases with the increase in ϕ [22] and is in agreement with our previous work [36, 37]. The larger dihedral angles for **a** and **b** isomers are mainly due to stereo-electronic effects.

The calculated dihedral angles ϕ_1 and ϕ_2 between *m*-phenylene and the two radical centers in the unsubstituted diradical are 26.43° and 26.56° as shown in Table 2. For substituents in the common *meta* position, these vary in a very narrow range, while for substituents in the common *ortho* positions, the dihedral angles become very large and vary widely. The factor of planarity can be defined by $\chi_p = \cos\phi_1\cos\phi_2$. χ_p Will be zero if one of the angles is 90°. But generally, ϕ_1 and ϕ_2 are changed together for maintain the symmetry of the molecule. The species are completely non-planar if $\chi_p = 0$, that is, $\phi_1 = \phi_2 = 90°$. Actually, χ_p becomes zero if one of the angles is 90°, but as it usually happens, both ϕ_1 and ϕ_2 increase simultaneously toward 90°. The molecular frame is planar if $\chi_p = 1$, that is, $\phi_1 = \phi_2 = 0$. This structural feature has limited the width of variation for all calculated coupling constants. In the case of a pronounced deviation from planarity, McConnell's formula [12] indicates an antiferromagnetic coupling, that is, a negative value for the magnetic coupling constant. The strength of the magnetic coupling would be linearly dependent on χ_p that describes the extent of conjugation between the spacer and the two radical centers. Variation of the calculated M06-2X magnetic coupling constant with χ_p is illustrated in Fig. 4a–c. The corresponding B3LYP plots are similar and are shown in the Supporting Information as Figure S1. The figures show linear plots with large positive slopes and small negative intercepts except for the (**c**) series where the slope is extra-large and the intercept is large negative. The (c) series differs as the coupling constants are considerably larger. The negative intercept confirms a switch from through-bond spin interaction to McConnell's through-space (spin-dipole–spin-dipole) interaction mechanism [12]. The intercept (that corresponds to $\phi_1 = \phi_2 = 90°$) is relatively large (-27.05 cm^{-1}) for common *meta* substitution that would hardly deflect the two NN rings when the latter are placed perpendicular to the *meta*-phenylene plane. An equal deflection of the two NN moieties leads to a smaller intercept (-3.28 cm^{-1}) for common *ortho* substitution. An unequal deflection spoils McConnell's interaction and

Table 2 Calculated NICS(1), average Wiberg bond index (BO) and the angles of twist (ϕ) for the diradicals in triplet state

Species	NICS(1)		ΔNICS(1)	BO	ϕ_1	ϕ_2
	Diradical[a]	Molecule[b]				
Unsubstituted	−9.43	−10.20	0.77	0.99	26.43	26.56
1a	−9.86		0.29	1.01	44.50	47.09
1b	−9.49	−10.15	0.66	1.03	25.79	43.44
1c	−8.91		1.24	1.04	27.05	29.20
2a	−9.47		0.92	1.02	42.54	52.09
2b	−9.37	−10.39	1.02	1.04	22.44	54.60
2c	−9.44		0.95	1.06	26.04	27.65
3a	−9.58		0.47	1.01	84.05	84.22
3b	−9.23	−10.05	0.82	1.04	25.49	61.04
3c	−9.41		0.64	1.05	25.76	25.76
4a	−9.60		0.70	0.95	50.12	46.72
4b	−9.54	−10.30	0.76	1.06	24.60	48.70
4c	−9.44		0.86	1.05	26.05	28.69
5a	−9.22		0.66	1.01	65.18	57.04
5b	−9.25	−9.88	0.63	1.03	20.81	65.68
5c	−9.02		0.86	1.06	26.68	28.02
6a	−8.78		1.04	1.03	35.20	67.80
6b	−8.80	−9.82	1.02	1.05	27.60	44.07
6c	−9.15		0.67	1.06	30.71	33.11
7a	−7.83		1.10	1.04	43.84	56.60
7b	−8.25	−8.93	0.68	1.06	25.82	51.71
7c	−8.75		0.18	1.05	32.42	32.51
8a	−9.19		0.44	0.99	83.13	83.06
8b	−8.83	−9.63	0.80	1.02	21.81	85.48
8c	−8.84		0.79	1.05	35.08	35.56
9a	−9.32		0.75	1.01	49.92	59.38
9b	−9.44	−10.07	0.63	1.04	22.72	57.50
9c	−9.22		0.85	1.04	27.05	27.18

[a] This work, [b] R-phenyl, Ref. [45]

gives rise to a vanishingly small antiferromagnetic interaction for *ortho–para* substitution (intercept ~ -0.65 cm^{-1}).

Wiberg bond order (BO) for the NN–phenylene connecting bond is greater than 1.0 in all cases except **4a** and **8a**. The larger BO (>1.0) indicates a larger double bond character and hence a greater conjugation, thus a larger *J*. As all calculated BOs are close to 1, they are not informative here.

3.4 Spin density and SOMO

It is a well-known fact that in the isolated NN radical, almost all the spin densities are equally shared by the NO groups [52, 53]. Mulliken population analysis of spin density in all the triplet diradicals reveals the same trend, that is, almost all the spin density is equally shared by the 4 NO fragments of the 2 NN moieties. A typical example is illustrated in Fig. 5a. In the BS state, again, almost all the spin densities reside on the 2 NO groups of each NN. However, the 2 NO groups have unequal spin population but of the same sign. A similar spin distribution is found in the other NN fragment, though with an overall opposite sign, as shown in Fig. 5b. The spin density diagrams clearly illustrate the spin alternation in the most stable state.

A diradical has two singly occupied molecular orbitals (SOMOs). According to Borden and Davidson [54, 55], a pair of disjoint SOMOs generally leads to a singlet ground state with negative *J*, whereas the non-disjoint SOMOs give rise to a triplet ground state. In Fig. 6, we illustrate the nature of SOMOs in the BS solutions of fluoro derivative (**3a**, **3b** and **3c**). The SOMOs for **3a** are manifestly disjoint, whereas **3b** and **3c** have obviously non-disjoint SOMOs. Indeed, we calculate a negative coupling constant for **3a** and positive *J* values for **3b** and **3c**. Taking the example of **3b**, we also show in this figure that the B3LYP SOMOs only slightly vary from the M06-2X SOMOs. However, the SOMO dictum is known to fail when the frame of conjugation of the diradical strongly deviates from planarity [21, 22].

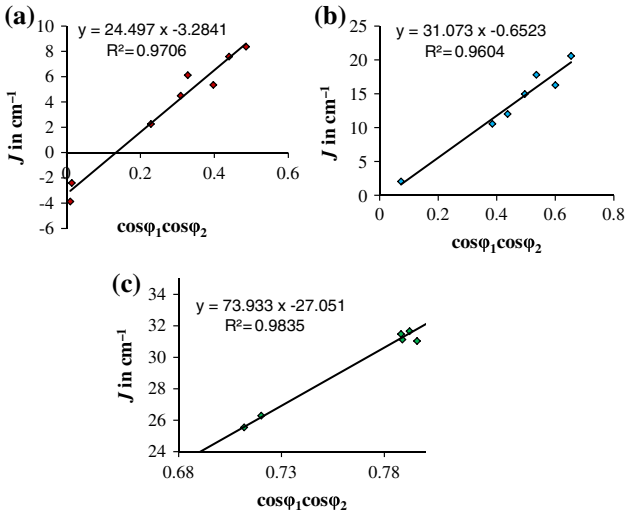

Fig. 4 Calculated J (M06-2X) versus χ_p, the factor of planarity: **a** common *ortho*: J (cm^{-1}) $= -3.28 + 24.50\chi_p$ (RMSD = 0.72); **b** *ortho–para*: J (cm^{-1}) $= -0.65 + 31.07\chi_p$ (RMSD = 1.12); **c** common *meta*: J (cm^{-1}) $= -27.05 + 73.93\chi_p$ (RMSD = 0.64)

3.5 Hammett constant

From the viewpoint of density functional theory (DFT), electronegativity can be defined as the negative of the partial derivative of the energy of an atomic or molecular system with respect to the number of electrons for a constant external potential [56]. Proft et al. [57] have carried out density functional calculations on different alkyl and alkyl alcohol groups and proposed that in gas phase, electron-withdrawing power increases with increasing electronegativity and hardness of the groups. Proft et al. [57] also verified that as the number of hydrogen atom increases, the electron-withdrawing power of the alkyl or alkyl alcohol group decreases.

Steric effect is too strong for (**a**) and (**b**) type substitutions, and the factor of planarity predominantly determines J in these two cases. Therefore, the variation of J with Hammett constant is checked only for the (**c**) type substitutions. From our previous calculation on Schlenk diradical [58] that is structurally similar to the present organic diradicals, we expect a linear dependence of J on the Hammett constants. This is indeed borne out in Fig. 7 where variation with σ_m is associated with a small slope (1.74) and small standard deviation (0.83). The slope ensures five points to be almost on the straight line. At $\sigma_m = 0$, the intercept 30.69 cm^{-1} may be compared with the input 32.7 cm^{-1} for hydrogen as substituent. Variation of J with Hammett constant shows the correlation of the strength of magnetic interaction with acidity, that is, the electron-withdrawing power of the substituent. This observation has theoretical importance as discussed in Ref. [58]. This effect is visible only for common *meta* position (**c**), but it is masked by steric factor for the other two locations (**a**) and (**b**).

3.6 Nucleus-independent chemical shift (NICS)

NICS is a measure of aromaticity. The significance of negative values of NICS indicates that the systems are

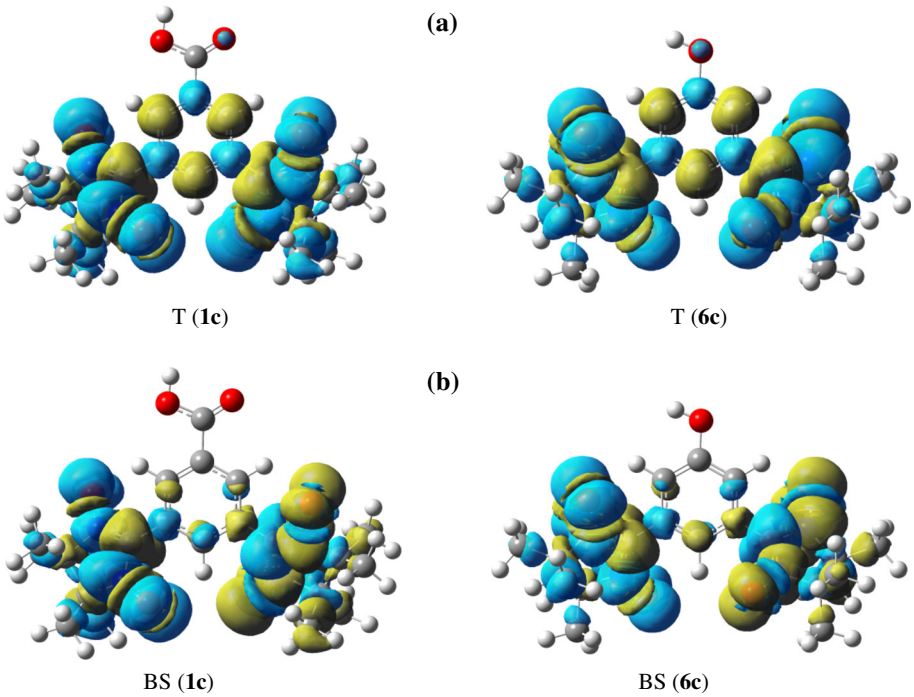

Fig. 5 Mulliken spin density plots (M06-2X) for **1c** and **6c** (**a**) in triplet (T) and (**b**) broken-symmetry (BS) solutions

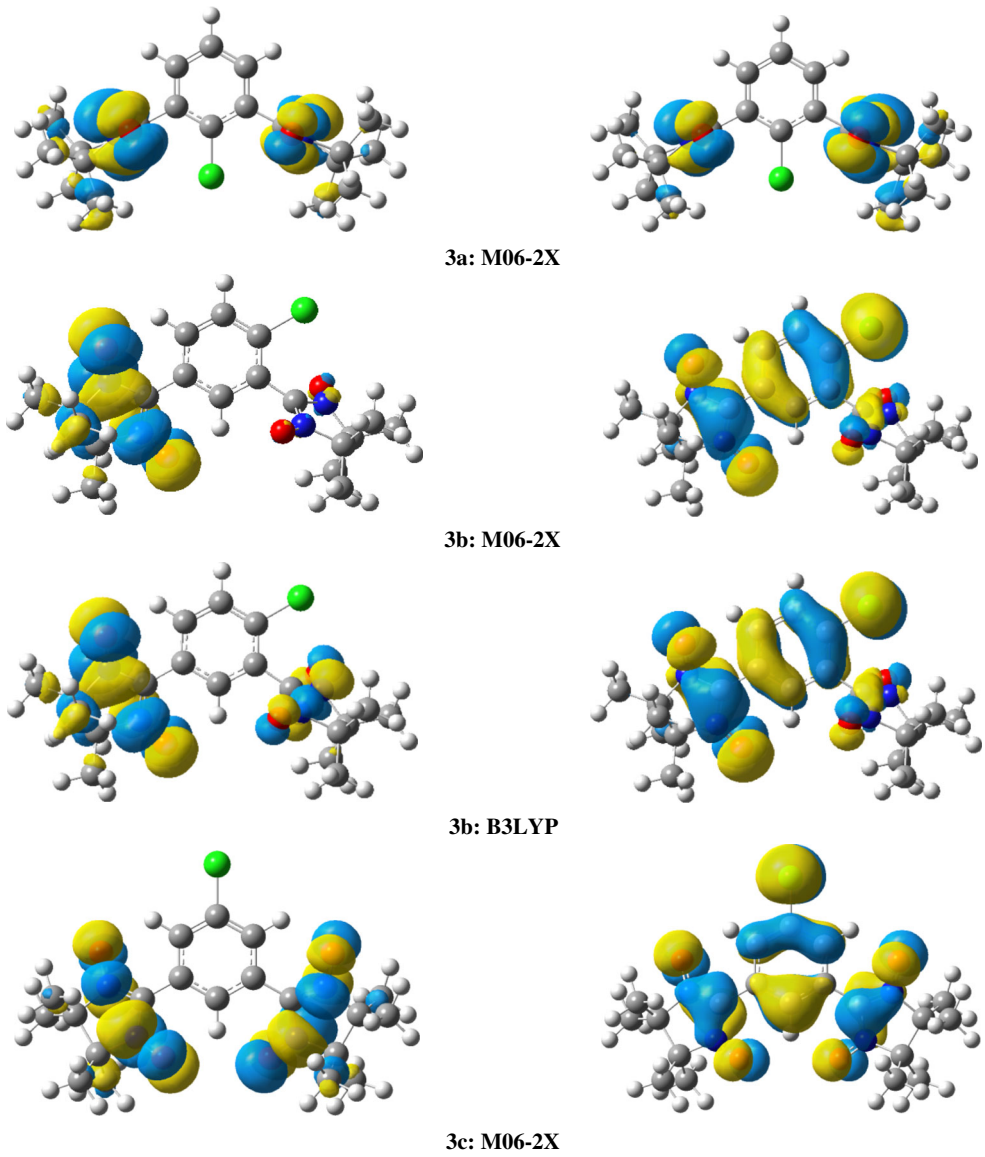

Fig. 6 SOMO plots for the broken-symmetry solutions of the fluorine derivatives of *m*-BNN (**3**). The SOMOs for **3a** are manifestly disjoint, whereas **3b** and **3c** have obviously non-disjoint SOMOs. As shown for **3b**, the B3LYP SOMOs show only a minor variation from the M06-2X diagrams

aromatic and positive values of NICS indicate that the systems are anti-aromatic [59]. The higher the negative value of NICS, the higher will be the aromatic character of any molecular system. Any system with zero NICS value means the system is completely non-aromatic. Schleyer et al. [60] proposed that NICS(1) gives some useful information about aromatic character of different hydrocarbons. The NICS(1) is nucleus-independent chemical shift calculated at a point 1 Å above the center of aromatic ring.

The NICS tensor and its isotropic average (simply, the chemical shift) represent fractional departures from the tensor or average for a reference substance, often tetramethyl silane (TMS). This reference has a C-13 nucleus thoroughly shielded by an almost perfectly spherical charge distribution. A negative value of the chemical shift is taken to imply de-shielding owing to departures from the spherical distribution. For ring systems, it is appealing to consider "ring current" that can define a local magnetic field by circulation of charge around the ring.

The computation of the chemical shift tensor rests on a perturbation-theoretical analysis. The first-order term, a property of the ground state, defines the diamagnetic portion. The second-order term defines the paramagnetic contribution. Its value depends in part on the energy gap between ground and triplet excited states, or more

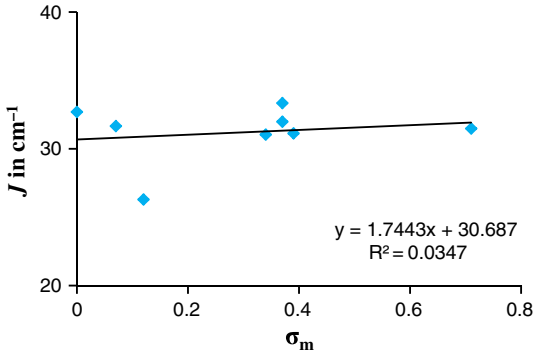

Fig. 7 Plot of calculated J (M06-2X) for type (**c**) species (common *meta* substitution) versus σ_m: $J\ (\mathrm{cm}^{-1}) = 1.74\sigma_m + 30.69$ (RMSD = 0.84)

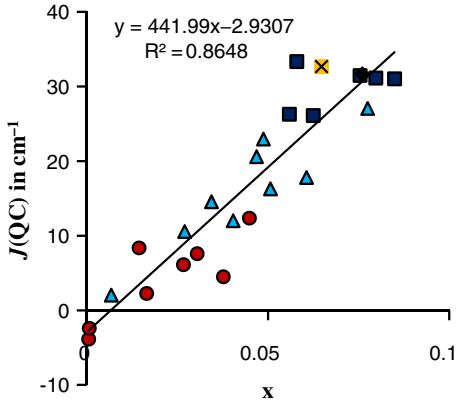

Fig. 8 Least square fitting of the calculated coupling constant with Eq. (6). The optimized parameters are $A = -442.0$ and $B = -2.931$, with $R^2 = 0.865$ and RMSD 4.31. The series of diradicals are indicated as **a** *red circle*, **b** *blue triangle* and **c** *black square*. The cross in *yellow* represents the unsubstituted *m*-BNN

approximately on the LUMO–HOMO energy gap of a closed-shell molecule. The stabilization characteristic of systems called aromatic is attended by a large LUMO–HOMO energy gap, and any feature of a particular molecule that changes this gap must affect the second-order term in the chemical shift. Thus, we imagine that elevating the HOMO (by a pi-donor) or depressing the LUMO (by a pi-acceptor) would have an adverse effect on the chemical shift. For a diradical, we have to deal with a pair of SOMOs instead of the doubly occupied and virtual couple. The SOMO energy difference (or the LUMO–HOMO energy gap of the coupler) can be viewed as the contributing factor.

3.6.1 Combined dependence

As the original Noodleman formula [31–33]

$$J = \frac{E(\mathrm{BS}) - E(T')}{1 + S_{ab}^2} \tag{4}$$

suggests, the evaluation of J would need a calculation of the overlap of magnetic orbitals Sab. This would provide a transparent intuitive interpretation. However, although identifying the magnetic orbitals is easy for transition metal complexes, it remains a non-trivial task for a moderately large organic diradical. The α-HOMO and β-HOMO in the BS solution may be taken as the magnetic orbitals: This has been attempted before for bis-NN diradicals with linear chain couplers and aromatic couplers, with partial success [37]. Still, the magnetic orbital overlap remains to be related to structural parameters such as BO and dihedral angle so as to generate a clear physical picture.

An alternative way of understanding was put forward by Hoffmann and his group back in 1968. Hoffmann et al. [61] contended that a triplet ground state is favored when the LUMO–HOMO energy gap is small. Later, an improvement was suggested by Hay et al. [62] that a departure from near degeneracy favors the singlet ground state,

$$E(T) - E(S) = -2K_{ab} + \frac{(\Delta\varepsilon_{ab})^2}{\mathrm{J}_{aa} - \mathrm{J}_{ab}},\ (K_{ab} > 0) \tag{5}$$

where J and K are direct and exchange integrals involving the SOMOs a and b. Again, this formula lacks a direct structural interpretation.

We are interested in a description of J in terms of structural characteristics such as those discussed in Ref. [63]. Coupling of spins would depend on the paramagnetic nature of the coupler. This coupling would be enhanced when there is strong overlap and good energy matching between the SOMOs of radical carriers and the orbitals of coupler. The overlap is strongly affected by geometry. An empirical formula was proposed by Ali et al. [64] for fused-ring couplers:

$$J = A\frac{\Delta\mathrm{NICS}(1)\cos\phi_1\cos\phi_2(\mathrm{WBO})}{\mathrm{NICS}(1)} + B \quad \text{in cm}^{-1} \tag{6}$$

In the original formula of Ref. [64], the term B was not considered; we add it here for the sake of convenience. Equation (6) reflects the interplay of influences for *m*-phenylene-coupled radical sites, regardless of substitution elsewhere on the coupler ring. It includes steric effects through their impact on the torsion angles between the pi system of the coupler and the pi system of the radical carriers. The fractional change in NICS acts as surrogate for the fractional paramagnetic nature of the coupler. Wiberg BO reflects the general strength of interaction between radical centers and *m*-phenylene pi system. The structural characteristics NICS(1), ΔNICS(1), WBO, ϕ_1 and ϕ_2 are listed in Table 2.

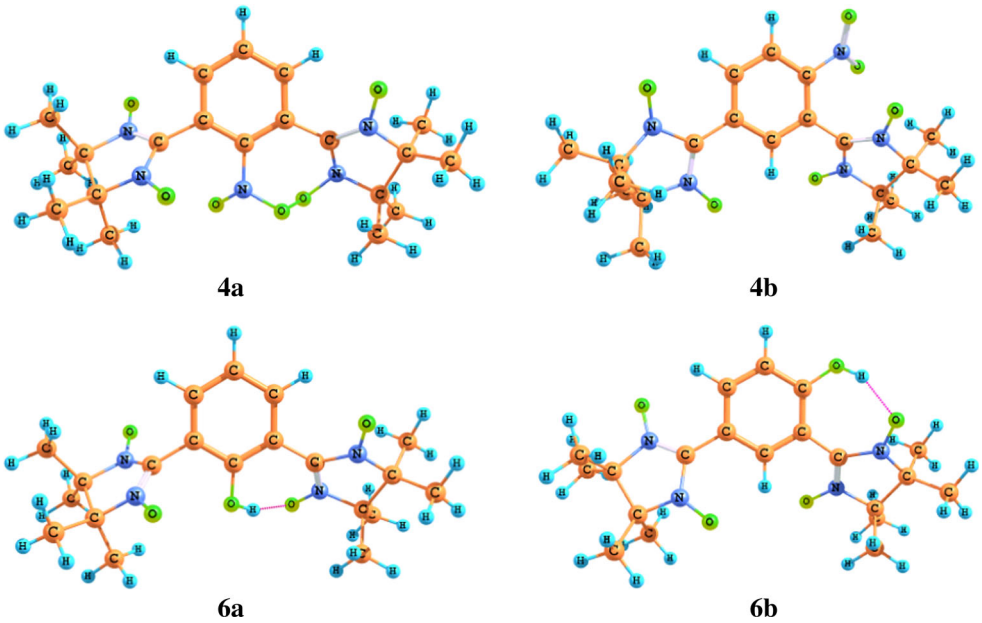

Fig. 9 The unique hydrogen bond formation observed for **4a**. No such bond is formed in **4b**. Intramolecular hydrogen bonding is found in **6a** and **6b**. (Similar hydrogen bonds are also observed for **1a**, **7a** and **7b**)

The formula (6) is unique in that it treats (**a**), (**b**) and (**c**) series of diradicals on the same footing, that is, using the same constants A and B. It recognizes the effects of substitution only in terms of the calculated structural characteristics in Table 2. A least square fit is depicted in Fig. 8. A fairly linear dependence is observed between the quantum chemical J and the empirical Eq. (6): $J(\mathrm{QC}) = Ax + B$. The optimized values are $A = -442.0$ and $B = -2.931$ with RMSD = 4.31. The slope A can be interpreted as an average proportionality constant for the three series of diradicals including the unsubstituted one, while the B value represents the average intercept that corresponds $\chi_p = 0$. In other words, B is the average coupling constant for the radical center planes being perpendicular to the coupler plane and is necessarily negative as discussed in Sect. 3.3 (spin dipolar interaction—the so-called McConnell mechanism—normally leading to antiferromagnetic interactions) and illustrated by Fig. 4.

For the systems studied here, we expect the effects of substitution to be smallest for the c-substituted sites, where the substituent would have electronic but no steric impact. The importance of steric effects would be more serious in b-substituted systems for which there is one *ortho* interaction, and still more severe for the a-substituted systems for which there are two *ortho* substitutions effective conjugation between pi coupler and radical sites.

First, we consider the impact of substitution on NICS(1) of the phenyl system. In the following statements, enhancing NICS makes the value more negative and makes the system more aromatic.

1. Substitutions that enhance NICS(1) on benzene: F > NO_2.
2. Substitutions that decrease NICS(1) on benzene: $NH_2 \gg$ phenyl > OH > Br.
3. Substitutions with little effect on NICS(1) on benzene: Cl, CH_3, COOH.

Introducing the NN radicals makes NICS(1) for *m*-phenylene more positive and diminishes the aromatic character.

The a-type (*ortho–ortho*) substitution has a major impact on torsion angles especially for phenyl and oddly for chloro groups. The J values are strikingly diminished by a-type substitutions, sometimes changing sign from positive to negative values (amino > phenyl > Cl). The a-type substitutions can either make NICS(1) more positive, reducing aromaticity (amino $\gg$ hydroxyl > phenyl and bromo), or make NICS(1) more negative, enhancing aromaticity (carboxyl $\gg$ chloro).

The c-type (common *meta*) substitutions have generally little effect on torsion angles. The c-type substitution generally enhances the Wiberg index slightly. There are small changes for R = phenyl and amino, tending to push them further out of alignment with *m*-phenylene ring, and diminishing J.

The b-type (*ortho–para*) substitution has a more dramatic effect on its *ortho* neighbor's torsion angle, than on the *para* NN. The effect on J is generally intermediate between c-type and a-type substitutions. For hydroxyl and amino, the impact is modest; for phenyl, the impact is large. The b-type substituents have puzzling consequences for NICS(1).

Para hydrogen bonding produces mostly structural effects such as a reduction in the twist angle ϕ as in **6a** and **6b** (Fig. 9), and also a small amount of spin delocalization

effect. The bulky phenyl group leads to an increase in the twist angle in its neighbor, (both ϕ_1 and ϕ_2 in **8a** and only ϕ_2 in **8b**). Thus, **8a** becomes antiferromagnetically coupled, and **8b** is only faintly ferromagnetic (see Tables 1 and 2).

4 Conclusions

The magnetic exchange coupling in 25 diradicals are predicted as ferromagnetic at UB3LYP/6–311+G(d,p), UB3LYP-D3/6–311+G(d,p) and M06-2X/6–311+G(d,p) levels. Species **3a** and **8a** are antiferromagnetically coupled. The substitution at the *meta* position of bis-NN-*m*-phenylene diradicals has little steric and hydrogen-bonding effects. In the case of a large twist of the planes of the spin sources from the plane of the coupler, the nature of interaction changes from ferromagnetic to antiferromagnetic. In these cases, the BO becomes small. The NICS value is found to decrease from the corresponding mono-substituted phenyl derivatives. The coupling constant is more or less linearly dependent on the product of (ΔNICS/NICS) and factor of planarity, with a small but distinctly negative intercept.

5 Supporting information

Log files of all calculations and Ref. [43] and [44]. The materials are available free of charge at http://pubs.acs.org.

Acknowledgments This work has been supported by Indo-Spain Collaborative Program in Science—Nanotechnology (DST Grant INT-Spain-P42-2012 and Spanish Grant PRI-PIBIN-2011-1028) and, in part, by Spanish MICINN through research Grant CTQ2012-30751 and by *Generalitat de Catalunya* through Grants 2009SGR1041 and XRQTC. Furthermore, SND and AKP are grateful to DST Grant SR-S1-PC-19-2010 for financial support of this work. I.A.L thanks Council of Scientific and Industrial Research for financial support, and FI acknowledges additional financial support through the 2009 ICREA Academia Award for Excellence in University Research. We acknowledge IIT Bombay computer center for making their facilities available to us.

References

1. Rajca A, Utamapanya S (1992) J Org Chem 57:1760
2. Wentrup C (2002) Science 295:1846
3. Rajca A, Shiraishi K, Pink M, Rajca S (2007) J Am Chem Soc 129:7232
4. Kahn O (1993) Molecular Magnetism, 2nd edn. Wiley, New York
5. Rajca A (1994) Chem Rev 94:871
6. Matsuda K, Matsuo M, Mizoguti M, Higashiguchi K, Irie M (2002) J Phys Chem B 106:11218
7. Catala L, Turek P, Moigne JL, Cian AD, Kyritsakas N (2000) Tetrahedron Lett 41:1015
8. Benelli C, Gatteschi D (2002) Chem Rev 102:2369
9. McWeeny R (1989) Pure Appl Chem 61:2087
10. Longuet-Higgins HC (1950) J Chem Phys 18:265
11. Ovchinnikov AA (1978) Theor Chim Acta 47:297
12. McConnell HM (1963) J Chem Phys 39:1910
13. Trindle C, Datta SN (1996) Int J Quantum Chem 57:781
14. Trindle C, Datta SN, Mallik B (1997) J Am Chem Soc 119:12947
15. Platz MS, Borden WT (1982) Diradicals, chap 8. Wiley, New York
16. Ioth K (1967) Chem Phys Lett 1:235
17. Dougherty DA (1990) Acc Chem Res 24:88
18. Takano Y, Onishi T, Kitagawa Y, Soda T, Yoshioka Y, Yamaguchi K (2000) Int J Quantum Chem 80:681
19. Ishida T, Kawakami T, Mitsubori S, Nogami T, Yamaguchi K, Iwamura H (2002) J Chem Soc Dalton Trans 60:3177
20. Ishida T, Mitsubori S, Nogami T, Takeda N, Ishikawa M, Iwamura H (2001) Inorg Chem 40:7059
21. Dvolaitzky M, Chiarelli R, Rassat A (1992) Angew Chem Int Ed Engl 31:180
22. Kanno F, Inoue K, Koga N, Iwamura H (1993) J Am Chem Soc 115:847
23. Fang S, Lee M, Hrovat DA, Borden WT (1995) J Am Chem Soc 117:6727
24. Mitani M, Mori H, Takano Y, Yamaki D, Yoshioka Y, Yamaguchi K (2000) J Chem Phys 113:4035
25. Mitani M, Yamaki D, Takano Y, Kitagawa Y, Yoshioka Y, Yamaguchi K (2000) J Chem Phys 113:10486
26. Zhang G, Li S, Jiang Y (2003) J Phys Chem A 107:5573
27. Reta Mañeru D, Pal AK, Moreira IPR, Datta SN, Illas F (2014) J Chem Theory Comput 10:335
28. Kamiyama K, Shiomi D, Hase S, Nishizawa M, Sato K, Kozaki M, Okada K, Takui T (2000) Appl Magn Reson 19:45
29. Hase S, Shiomi D, Sato K, Takui T (2001) J Mater Chem 11:756
30. Shiomi D, Tamura M, Sawa H, Kato R, Kinoshita M (1993) J Phys Soc Jpn 62:289
31. Noodleman L (1981) J Chem Phys 74:5737
32. Noodleman L, Baerends EJ (1984) J Am Chem Soc 106:2316
33. Noodleman L, Peng CY, Case DA, Mouesca JM (1995) Coord Chem Rev 144:199
34. Ginsberg AP (1980) J Am Chem Soc 102:111
35. Noodleman L, Davidson ER (1986) Chem Phys 109:131
36. Ali ME, Vyas S, Datta SN (2005) J Phys Chem A 109:6272
37. Ali ME, Datta SN (2006) J Phys Chem A 110:2776
38. Yamaguchi K, Takahara Y, Fueno T, Nasu K (1987) Jpn J Appl Phys 26:L1362
39. Yamaguchi K, Jensen F, Dorigo A, Houk KN (1988) Chem Phys Lett 149:537
40. Caballol R, Castell O, Illas F, Malrieu JP, Moreira IPR (1997) J Phys Chem A 101:7860
41. Moreira IPR, Illas F (2006) Phys Chem Chem Phys 8:1645
42. Vyas S, Ali ME, Hossain E, Patwardhan S, Datta SN (2005) J Phys Chem A 109:4213
43. Frisch MJ, Trucks GW, Schlegel HB, Scuseria GE, Robb MA, Cheeseman JR, Montgomery JA Jr, Vreven T, Kudin KN, Burant JC et al (2003) Gaussian 03. Gaussian Inc, Pittsburgh
44. Gaussian 09, Revision A.1, Frisch MJ, Trucks GW, Schlegel HB, Scuseria GE, Robb MA, Cheeseman JR, Scalmani G, Barone V, Mennucci B, Petersson GA et al. (2009) Gaussian, Inc., Wallingford
45. Chen Z, Wannere CS, Corminboeuf C, Puchta R, Schleyer PVR (2005) Chem Rev 105:3842
46. Wiberg K (1968) Tetrahedron 24:1083
47. Glendening ED, Reed AE, Carpenter JE, Weinhold F (1990) QCPE Bull 10:58
48. Weinhold F, Landis CR (2001) Chem Educ Res Pract Eur 2:91
49. Kitagawa Y, Saito T, Ito M, Shoji M, Koizumi K, Yamanaka S, Kawakami T, Okumura M, Yamaguchi K (2007) Chem Phys Lett 442:445

50. Malrieu JP, Trinquier GJ (2012) J Phys Chem A 116:8226
51. Saito T, Thiel WJ (2012) J Phys Chem A 116:10824
52. Zheludev A, Barone V, Bonnet M, Delley B, Grand A, Ressouche E, Rey P, Subra R, Schweizer J (1994) J Am Chem Soc 116:2019
53. Novoa JJ, Lafuente P, Deumal M, Mota F (2002) Magnetism: molecules to materials IV, vol 3. Wiley, New York, p 78
54. Borden WT, Davidson ER (1977) J Am Chem Soc 99:4587
55. Constantinides CP, Koutentis PA, Schatz J (2004) J Am Chem Soc 126:16232
56. Parr RG, Donnelly RA, Levy M, Palke WE (1978) J Chem Phys 68:3801
57. Proft FD, Langenaeker W, Geerlings P (1995) Tetrahedron 51:4021
58. Latif IA, Hansda S, Datta SN (2012) J Phys Chem A 116:8599
59. Schleyer PVR, Maerker C, Dransfeld A, Jiao AH, Hommmes NJRVE (1996) J Am Chem Soc 118:6317
60. Schleyer PVR, Jiao H, Hommes NJRVE, Malkin VG, Malkina OL (1997) J Am Chem Soc 119:12669
61. Hoffmann R, Imamura A, Hehre WJ (1968) J Am Chem Soc 90:1499
62. Hay PJ, Thibeault JC, Hoffmann R (1975) J Am Chem Soc 97:4884
63. Datta SN, Trindle CO, Illas F (2013) Theoretical and computational aspects of magnetic organic molecules, vol 6. Imperial College Press, London
64. Ali ME, Datta SN (2006) J Phys Chem A 110:13232